



HAL
open science

Novel ketone derivatives based photoinitiating systems for free radical polymerization under mild conditions and 3D printing

Yangyang Xu, Guillaume Noirbent, Damien Brunel, Zhaofu Ding, Didier Gimes, Yijun Zhang, Shaohui Liu, Bernadette Graff, Pu Xiao, Frédéric Dumur, et al.

► **To cite this version:**

Yangyang Xu, Guillaume Noirbent, Damien Brunel, Zhaofu Ding, Didier Gimes, et al.. Novel ketone derivatives based photoinitiating systems for free radical polymerization under mild conditions and 3D printing. *Polymer Chemistry*, 2020, 11 (36), pp.5767-5777. 10.1039/d0py00990c . hal-02946028

HAL Id: hal-02946028

<https://hal.science/hal-02946028>

Submitted on 22 Sep 2020

HAL is a multi-disciplinary open access archive for the deposit and dissemination of scientific research documents, whether they are published or not. The documents may come from teaching and research institutions in France or abroad, or from public or private research centers.

L'archive ouverte pluridisciplinaire **HAL**, est destinée au dépôt et à la diffusion de documents scientifiques de niveau recherche, publiés ou non, émanant des établissements d'enseignement et de recherche français ou étrangers, des laboratoires publics ou privés.

Novel ketone derivatives based photoinitiating systems for free radical polymerization under mild conditions and 3D printing

Yangyang Xu,^{a,b*} Guillaume Noirbent,^c Damien Brunel,^c Zhaofu Ding,^a Didier Gigmes,^c Yijun Zhang,^b Shaohui Liu,^b Bernadette Graff,^b Pu Xiao,^{d*} Frédéric Dumur^{c*} and Jacques Lalevée^{b*}

^aCollege of Chemistry and Materials Science, Anhui Normal University, South Jiu Hua Road 189, Wuhu 241002, P. R. China. E-mail: ahnuxyy@ahnu.edu.cn

^bInstitut de Science des Matériaux de Mulhouse, IS2M-UMR CNRS 7361, UHA, 15, rue Jean Starcky, Cedex 68057 Mulhouse, France. E-mail: jacques.lalevee@uha.fr

^cAix Marseille Univ, CNRS, ICR UMR 7273, F-13397 Marseille, France. E-mail: Frederic.dumur@univ-amu.fr

^dResearch School of Chemistry, Australian National University, Canberra, ACT 2601, Australia. E-mail: pu.xiao@anu.edu.au

Abstract: Photopolymerization of acrylates under mild conditions is promising for not only academic research, but also for industrialization applications. However, it still remains a huge challenge to develop effective photoinitiators or photoinitiating systems for the free radical polymerization of acrylates upon visible light-emitting diode (LED) irradiation. In this work, twelve novel ketone derivatives containing either tertiary amines or anthracenes as peripheral substituting groups (noted as Ami-1~Ami-6 and Anth-1~Anth-6) were elaborately synthesized and proposed for the polymerization of di(trimethylolpropane) tetraacrylate (TA), a tetrafunctional polyether acrylate, in both thin and thick films conditions under the LED@405 nm irradiation. In combination with an amine and an iodonium salt (Iod), these ketones could form distinct three-component photoinitiating systems, among which the Ami-2/amine/Iod system could lead to the highest final conversion of acrylates in the thick film (~1.4 mm) condition while Ami-6/amine/Iod system could induce the highest final conversion of acrylates in the thin film (~25 μm) condition. Photosensitivity of Ami-2 and Ami-6 was systematically investigated by the steady state photolysis and fluorescence quenching experiments. Finally, photocuring 3D printing technique was applied to TA, and both Ami-2 and Ami-6 based photoinitiating systems could be used to fabricate macroscopically tridimensional patterns with excellent spatial resolution.

1. Introduction

Generally speaking, light induced polymerization or photopolymerization technique can transform a specially formulated reactive liquid (*e.g.* polymerizable monomer or oligomer) into a solid material through photocuring process activated upon light exposure. And usually, the photopolymerization reaction can be initiated by the type I (mono-component initiating system) or type II (bi-component or multiple-component initiating system) photoinitiators, of which the latter is especially versatile.¹⁻⁵ Thanks to these intrinsic advantages, such as fast polymerization kinetics, mild reaction conditions, **environmentally friendly polymerization process**, its economic aspect with

less energy consumed, as well as an excellent spatial and temporal control, photopolymerization reactions have been widely studied and developed over the past decades. Now, the photopolymerization technique is attracting a widespread attention in both traditional and high-tech areas, including coatings, paints, inks, adhesives, microlithography, microelectronics, dentistry, and photocuring 3D-printing...to name just a few.⁶⁻¹⁰

For the moment, the majority of the commercially available photoinitiators are UV sensitive, although the UV light is harmful for the environment and human well-beings.^{11,12} In this context, the exploration of alternative safe irradiation sources based on near-UV and visible light is a cherished desire for mild photopolymerization conditions. Now, the usage of visible light-emitting irradiation sources such as light emitting diode (LED) has appealed a huge interest and attention. The advantageous features of LEDs include low energy consumption and costs, no ozone release, fewer UV rays and heat generation, easy and safe operation, little maintenance, long lifetime as well as light intensity tunability.¹³⁻¹⁵ However, the availability of LED curable formulations for photopolymerization is still very limited. Therefore, the development of effective photoinitiators or photoinitiating systems sensitive to LED irradiation is of utmost importance and urgent necessity.

The free radical polymerization of acrylates occupies a major part in polymer synthesis field for not only academic research, but also for industrialization applications.¹⁶⁻¹⁸ Ketone scaffold-based chromophores are well known for their light absorption properties at the near-UV and visible range, but reports mentioning their uses for the LED activated photopolymerization are still scarce.^{19,20}

In this work, twelve different ketone derivatives differing by the central cyclohexanones and the peripheral substituting moieties were introduced and their photoinitiating abilities upon visible LED irradiation were investigated in detail. In combination with an amine and an iodonium salt, these ketones could form three-component type II photoinitiating systems, which could be used for the free radical polymerization of acrylates. Photopolymerization kinetics of acrylates in the presence of ketones based photoinitiating systems were studied by real time Fourier transform infrared spectroscopy, and the photoreactivity of these ketones was investigated through UV-vis absorption and fluorescence spectra. A practical application of the three-component photoinitiating systems based on ketones for free radical polymerization of acrylates was further demonstrated with the 3D printing experiments to produce macroscopically tridimensional patterns. Remarkably, none of these ketone derivatives has ever been reported or used for the photopolymerization prior to this work, especially upon visible LED.

2. Experimental section

2.1. Materials

All the twelve different ketones investigated in this work were synthesized according to procedures described in detail in the ESI (see Scheme S1), and their chemical structures were depicted in Scheme 1. Ethyl 4-(dimethylamino)benzoate (commercial name: EDB) and the iodonium salt (Iod) di-*tert*-butyl-diphenyl iodonium

hexafluorophosphate (commercial name: Speedcure 938) were obtained from Lambson Ltd. Di(trimethylolpropane) tetraacrylate (TA, commercial name: Ebecryl 40), a tetrafunctional polyether acrylate, was purchased from Allnex and used as the benchmark monomer for the free radical photopolymerization. All these commercially available chemical compounds were selected with the highest purity and used as received without further purification, as shown in Scheme 2.

2.2. Formulation preparation

Ketones, amine and iodonium salt were successfully added into colorless TA, and the weight percent of the three-component photoinitiating system was set as 0.1%/2%/2% (w/w/w), which was calculated from the monomer content (Table S1). Then, a homogeneous resin could be produced upon the mechanical mixing by a SpeedMixer (DAC 150.1 FVZ-K) with rotation speed at 1200 rpm for several minutes (Fig. S1).²¹ The prepared formulation was stored in the dark at room temperature before photo-irradiation to avoid pre-polymerization.

2.3. Irradiation source

A visible LED with maximum emission wavelength at 405 nm was utilized as the irradiation source for both the free radical polymerization and steady state photolysis experiments. The incident light intensity at sample surface was set about 110 $\text{mW}\cdot\text{cm}^{-2}$.

2.4. Free radical photopolymerization

The free radical photopolymerization of TA was carried out in laminate (the formulation is sandwiched between two polypropylene films to minimize the O_2 inhibition effect during the photopolymerization) at room temperature. For the thick samples, the prepared photosensitive formulations were deposited into a rounded plastic mold of 1.4 mm thickness and 7 mm diameter. For the thin samples, one drop resin was directly deposited between two polypropylene films with thickness about 25 μm . Evolution of the C=C double bond content in TA was continuously followed using real time Fourier transform infrared spectroscopy (RT-FTIR, JASCO FTIR 4100) at about 4740 cm^{-1} for thick samples and 1630 cm^{-1} for thin samples (NIR was used to follow the photopolymerization process for thick samples), respectively.^{22,23} The final conversion (FC) of the reactive acrylate groups at irradiation time t during the photopolymerization was calculated as

$$\text{FC} = (A_0 - A_t)/A_0 \times 100\%$$

where A_0 is the initial peak area of the functional acrylate groups before irradiation, and A_t is the corresponding peak area after LED irradiation for a given time t .^{24,25}

2.5. UV–visible absorption and photolysis experiments

The UV–visible absorption properties of the ketones and the steady state photolysis experiments were both studied by JASCO V730 UV–visible spectrometer using acetonitrile as the solvent, the specific conditions are given in the figure captions.

2.6. Fluorescence quenching experiments

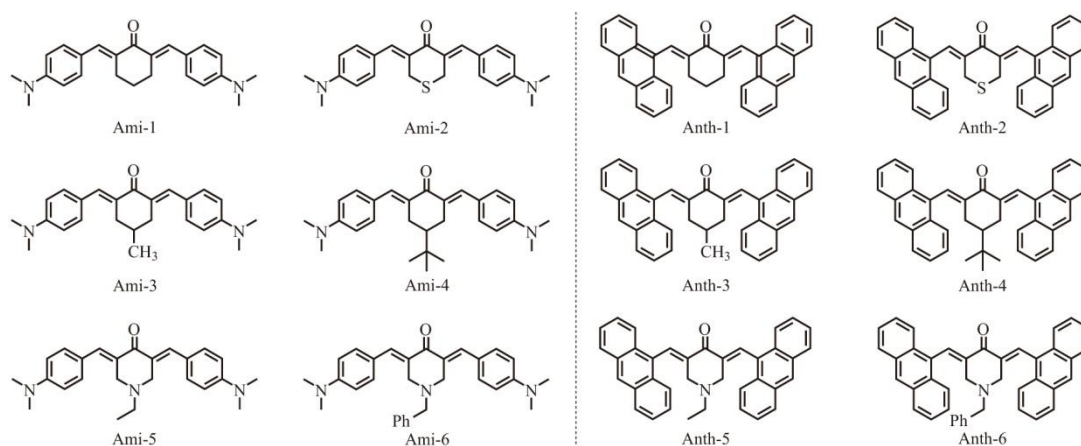
The fluorescence properties of the different ketones dissolved in acetonitrile were studied with a JASCO FP-6200 spectrofluorimeter, the specific conditions are given in the corresponding figures.

2.7. Molecular modeling

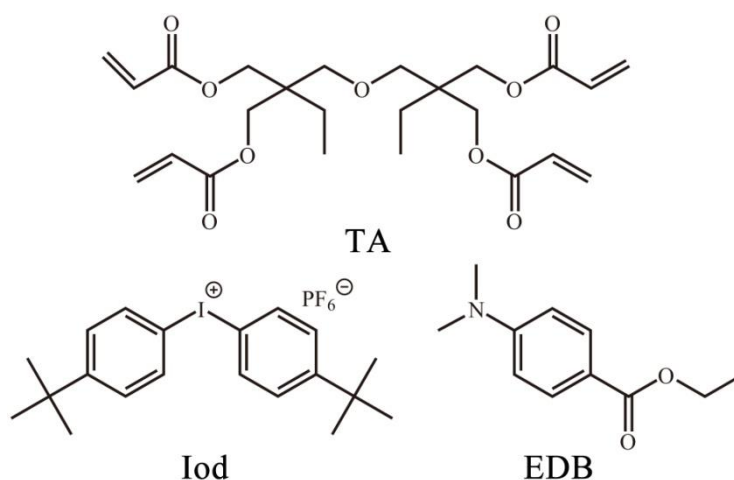
Frontier molecular orbital calculations were executed through the Gaussian 03 suite of programs. The highest occupied molecular orbitals (HOMOs) and lowest unoccupied molecular orbitals (LUMOs) of the ketone derivatives were calculated with the time-dependent density functional theory (TD-DFT) at the UB3LYP/6-3G* level of theory.

2.8. 3D printing experiments

The prepared photosensitive formulations were deposited into a homemade glass square groove with ~1 mm or ~2 mm thickness. A laser diode@405 nm (Thorlabs) was computer programmed and used for the spatially controllable irradiation. For the sake of comparison with the RT-FTIR kinetic experiments, the intensity of the laser on the sample surface was also set about 110 mW cm⁻², and the spot size of the irradiation laser was about 50 μm. The laser writing experiment of the resin was carried out under air at room temperature. And the generated three-dimensional patterns were observed and analyzed by a numerical optical microscope (DSX-HRSU, OLYMPUS corporation).



Scheme 1 Chemical structures of the twelve newly proposed ketone derivatives.

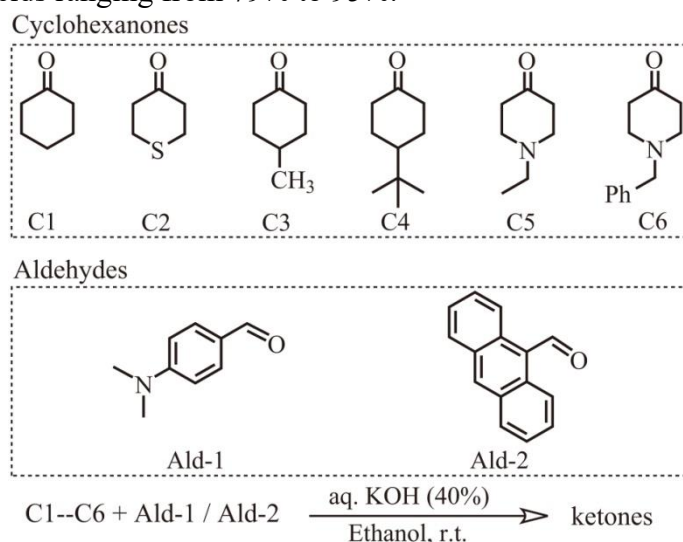


Scheme 2 Chemical structures of the acrylate monomer (TA) and photo-additives (Iodonium salt/Iod and EDB).

3. Results and discussion

3.1. Synthesis of the twelve ketones

According to their different peripheral substituting groups (tertiary amine or anthracene), these twelve ketone derivatives could be categorized into two distinct series: Ami-(1~6) and Anth-(1~6). General synthetic routes towards the targeted ketones are outlined in Scheme 3, and the detailed synthetic procedures and structure characterizations for each ketone are presented in the ESI. Briefly, these twelve ketones were obtained by a Knoevenagel reaction opposing 4-dimethylaminobenzaldehyde or anthracene-9-carbaldehyde to the appropriate cyclohexanones under strongly basic conditions (aq. KOH 40%).²⁶⁻²⁸ All ketone products were isolated and purified as solids with reaction yields ranging from 79% to 95%.



Scheme 3 Synthetic routes to the twelve ketone derivatives.

3.2. Light absorption properties of the investigated ketones

UV-visible absorption spectra of the new ketone-based photoinitiators were recorded in acetonitrile and the spectra are depicted in Fig. 1 and Fig. S2. Absorption maxima (λ_{max}) and molar extinction coefficients at λ_{max} (*i.e.* ϵ_{max}) and at 405 nm (*i.e.* $\epsilon_{405 \text{ nm}}$) are summarized in the Table 1, respectively. In terms of absorption property, a strong absorption in the visible region was found for the tertiary amine substituted ketone derivatives (Ami-1~Ami-6). λ_{max} of the tertiary amine substituted ketones varied between 430 and 440 nm, and their corresponding ϵ_{max} ranged from 40000 to 50000 $\text{M}^{-1} \text{cm}^{-1}$. Interestingly, all of these six ketones also showed a relatively strong absorption at 405 nm with $\epsilon_{405 \text{ nm}}$ in the range from 30000 to 39000 $\text{M}^{-1} \text{cm}^{-1}$. Among all the six tertiary amine substituted ketone derivatives, Ami-3 possessed the highest $\epsilon_{405 \text{ nm}}$ (38400 $\text{M}^{-1} \text{cm}^{-1}$), while ketone Ami-6 showed the lowest $\epsilon_{405 \text{ nm}}$ (30000 $\text{M}^{-1} \text{cm}^{-1}$). On the contrary, a strong absorption in the UV region was characterized for the anthracene substituted ketone derivatives (Anth-1~Anth-6). All of these six ketones had the same λ_{max} at about 250 nm, while the corresponding ϵ_{max} differed from 80000 to 180000 $\text{M}^{-1} \text{cm}^{-1}$. $\epsilon_{405 \text{ nm}}$ of these anthracene substituted ketones are in the range between 5000 and 12000 $\text{M}^{-1} \text{cm}^{-1}$, which are much lower than those of their tertiary amine substituted ketone counterparts. According to their UV-visible absorption spectra, absorption properties of these twelve ketones differed dramatically, which is possibly caused by the different peripheral substituting groups, despite the various structures of the central

cyclohexanone cores. And compared with the anthracene substituted ketone derivatives (Anth-1~Anth-6), the tertiary amine substituted ketones (Ami-1~Ami-6) could ensure a good overlap with the emission spectra of the visible LED (LED@405 nm used in this work), rather than the conventional but harmful UV light.

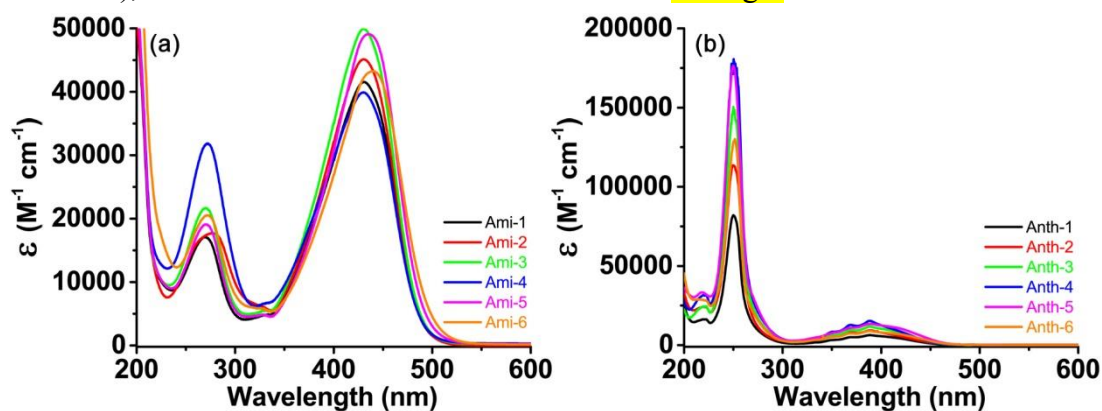


Fig. 1 UV-visible absorption spectra of the twelve ketones dissolved in acetonitrile.

Table 1 Light absorption properties of the twelve different ketones: absorption maxima wavelength (λ_{\max}) as well as the molar extinction coefficients at λ_{\max} (ϵ_{\max}) and at 405 nm ($\epsilon_{405 \text{ nm}}$), respectively.

	λ_{\max} (nm)	ϵ_{\max} ($\text{M}^{-1} \text{cm}^{-1}$)	$\epsilon_{405 \text{ nm}}$ ($\text{M}^{-1} \text{cm}^{-1}$)
Ami-1	430	41600	31900
Ami-2	430	45300	35000
Ami-3	431	49900	38400
Ami-4	430	40000	31900
Ami-5	436	49200	34200
Ami-6	440	43300	30000
Anth-1	250	81800	5400
Anth-2	250	113300	7400
Anth-3	250	149600	9900
Anth-4	250	178400	11500
Anth-5	250	175900	12000
Anth-6	250	129500	7800

TD-DFT theoretical calculations were performed to predict the frontier molecular orbitals of these ketone photoinitiators. For amine substituted ketone derivatives (Ami-1~Ami-6), charge transfer transitions are noted between the highest occupied molecular orbital (HOMO) and the lowest unoccupied molecular orbital (LUMO) localized onto two different moieties (Fig. 2 and Fig. S3). Conversely, for the anthracene substituted ketones (Anth-1~Anth-6), such a charge transfer character is not really observed.

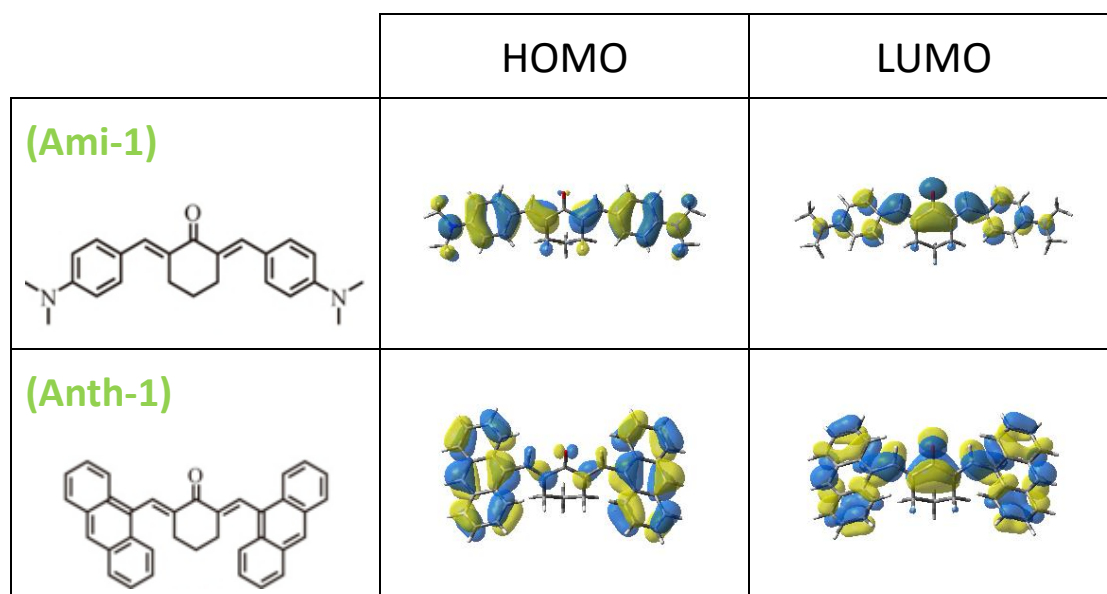


Fig. 2 Frontier molecular orbitals (HOMOs and LUMOs) of a selection of ketone derivatives investigated in this work (for the other ketones see in supporting information).

3.3. Photoinitiating ability of the ketones based three-component systems for the free radical polymerization of acrylate

TA (Scheme 2), a tetrafunctional polyether acrylate, is characterized by a mild odor, light color and low viscosity (110-210 mPa/s at 25°C). Our previous research has demonstrated that neither amine nor diphenyliodonium salt alone could initiate the free radical photopolymerization of acrylates (conversion~0%).²⁹ Therefore, in this work, the ketone/amine/Iod (0.1/2%/2%, w/w/w) combinations forming the different three-component photoinitiating systems were proposed and developed for the free radical polymerization of TA upon 405 nm LED irradiation at room temperature. Here, the ketones acted as the photoinitiators, amine (EDB, electron donor) and iodonium salt (Iod; Speedcure 938, electron acceptor) acted as co-initiator or photo-additive respectively. Initiating abilities of the different ketones-based photoinitiating systems for the free radical polymerization of TA monomers were investigated in both thick and thin films conditions. Typical functional acrylate conversion against LED irradiation time profiles were obtained by following the RT-FTIR characterization and given in Fig. S4 and Fig. S5. And the final acrylate function conversions (FCs) in the presence of different ketone/amine/Iod photoinitiating systems are summarized and compared in Table 2. On the one hand, photopolymerization of thick films (1.4 mm thickness plastic mold) furnished FCs for the acrylate monomer varying from 40% to 90% with different ketones-based photoinitiating systems. Both Anth-1/amine/Iod and Ami-2/amine/Iod three-component systems could induce the highest FC, which is about 90%. Meanwhile, Anth-2/amine/Iod and Anth-5/amine/Iod system could induce the lowest FC, which is only 41%. On the other hand, during the photopolymerization of thin films (~25 μm, the thickness is controlled from the FTIR spectra of the formulation), the FCs of acrylates varied between 40% and 80% in the presence of different ketone/amine/Iod three-component systems. Both Ami-6 and Anth-6 based photoinitiating system could

lead to the highest FC, which is about 76%, while Ami-1 based photoinitiating system could induce the lowest FC, which is only about 43%. In general, compared with the anthracene-substituted ketones, the tertiary amine-substituted ketones illustrated higher polymerization rates as shown by the curve slopes and the much shorter inhibition time in the photopolymerization profiles, thus demonstrating the higher photoinitiating efficiency for the free radical polymerization of acrylates.

Table 2 Final conversions (FCs) for reactive acrylates of TA in thick and thin films conditions upon exposure to LED@405 nm for 400 s in the presence of ketone/amine/Iod (0.1%/2%/2%, w/w/w) three-component photoinitiating systems, respectively.

FCs (in thick)	Ami-1	Ami-2	Ami-3	Ami-4	Ami-5	Ami-6
	~84%	~90%	~84%	~88%	~86%	~83%
	Anth-1	Anth-2	Anth-3	Anth-4	Anth-5	Anth-6
	~90%	~41%	~68%	~81%	~41%	~53%
FCs (in thin)	Ami-1	Ami-2	Ami-3	Ami-4	Ami-5	Ami-6
	~43%	~67%	~56%	~58%	~63%	~76%
	Anth-1	Anth-2	Anth-3	Anth-4	Anth-5	Anth-6
	~66%	~68%	~60%	~74%	~73%	~76%

The different photoinitiating abilities of these ketones are probably correlated with their different chemical structures with varied central cyclohexanone cores and peripheral substituting groups. Specifically, six representative polymerization kinetics profiles are depicted in Fig. 3 for the photopolymerization of TA in either thick or thin films conditions. And these six different ketone/amine/Iod three-component systems are selected because of their high polymerization rates in the photopolymerization profiles (Table S2). As shown in Fig. 3a, Ami-1, Ami-2 and Anth-1 based photoinitiating systems are presented for the free radical polymerization of acrylates in thick films condition. FCs of these three profiles are over 84%, and the different starting time for the polymerization is probably ascribed to the re-oxygenation effect, especially for the initiating system based on Anth-1. The polymerization only starts (this corresponds to the inhibition period) when oxygen is consumed. Meanwhile, for the free radical polymerization of acrylates in thin films, Ami-3, Ami-5 and Ami-6 based photoinitiating systems are presented in Fig. 3b. All of these three ketones could initiate the photopolymerization immediately upon LED without delay, demonstrating that the re-oxygenation effect could be neglected in the case of the thin films condition. And among the three ketones-based photoinitiating systems in thin films, the Ami-6-based photoinitiating system could induce the highest FC value (76%) of acrylates, Ami-5 could induce the medium FC value (63%), while Ami-3 could induce the lowest FC value (56%). Noticeably, Ami-4-based photoinitiating system could respectively induce similar polymerization profiles with Ami-2 in thick films and with Ami-3 in thin films, which is not shown in Fig. 3.

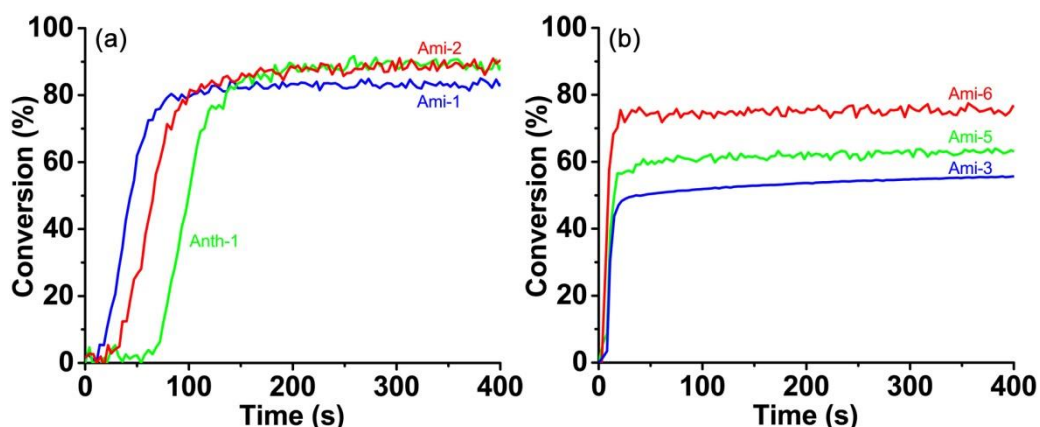


Fig. 3 Photopolymerization profiles of TA (acrylate function conversion vs. irradiation time) upon exposure to a LED@405 nm in the presence of ketone/amine/Iod (0.1%/2%/2%, w/w/w) three-component photoinitiating systems: (a) in thick films (thickness \approx 1.4 mm), and (b) in thin films (thickness \approx 25 μ m), respectively.

Since Ami-2/amine/Iod and Ami-6/amine/Iod three-component photoinitiating systems, respectively, could induce the highest FCs of acrylates in thick and thin films conditions, the IR spectra recorded before and after polymerization for TA with these two ketone-based photoinitiating systems are compared in Fig. 4. For the photopolymerization in thick films upon LED@405 nm irradiation, a dramatic intensity decline would be observed for the acrylate stretching C=C bond at 4740 cm^{-1} in the presence of Ami-2 based photoinitiating system (Fig. 4a).²² And for the photopolymerization in thin films under the same LED irradiation, also a dramatic intensity decline would be observed for the acrylate stretching C=C bond at 1630 cm^{-1} in the presence of Ami-6 based photoinitiating system (Fig. 4b).^{23,30} It's worth mentioning that the photo-additives, amine and iodonium salt, also play a very important role in the photoinitiating system. As illustrated in Fig. S6 and Table S3, neither Ami-2 nor Ami-6 alone can effectively initiate the free radical polymerization of TA in thick films. And the FCs of acrylates polymerized in thin films initiated by ketones alone are much lower than those by the corresponding ketone/amine/Iod three-component photoinitiating systems. All the above results indicated that, in combination with amine and iodonium salt, the ketone derivatives could be excellent candidates as photoinitiators for the free radical polymerization of acrylates under mild conditions.

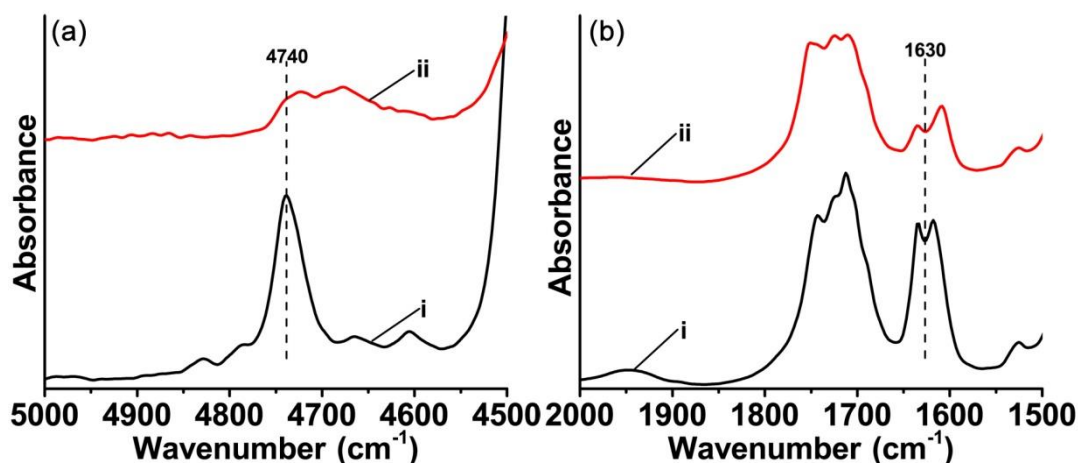


Fig. 4 IR spectra recorded (i) before and (ii) after polymerization of TA upon exposure to a LED@405 nm in the presence of (a) Ami-2/amine/Iod in thick films condition and (b) Ami-6/amine/Iod in thin films condition, respectively.

3.3. Steady state photolysis of Ami-2 and Ami-6

In order to investigate the photoreactivity of ketones, steady state photolysis experiments for the different ketones in the presence of photo-additives (amine and iodonium salt) were carried out. Since Ami-2 and Ami-6 based photoinitiating systems could induce the highest FCs for the free radical polymerization of acrylates in thick and thin films conditions, respectively, these two ketones were selected for the steady state photolysis characterization using a UV-visible spectrometer. The UV-vis absorption spectra of Ami-2 and Ami-6 in combination with amine (EDB) upon a 405 nm LED irradiation are presented in Fig. 5. Before irradiation, Ami-2 and Ami-6 both showed a strong absorbance in the 350-550 nm range, and their maximum absorbance peaks appeared at 426 nm and 438 nm, respectively. However, along with the increasing irradiation time of LED@405 nm, an apparent and successive intensity decline was observed for both Ami-2/amine and Ami-6/amine two-component systems (Fig. 5a, 5c). Precisely, the percentage consumption of ketones against LED irradiation time was calculated according to the spectral decrement of the maximum absorbance in the UV-vis absorption spectra. As shown in Fig. 5b, a nonlinear growth for the percentage consumption of Ami-2, in combination with amine, was detected against the irradiation time with LED@405 nm. And after the LED irradiation for just 6 min, the final percentage consumption of Ami-2 reached about 27%. Similarly, the percentage consumption of Ami-6, in combination with amine, also showed a nonlinear relationship with the LED@405 nm irradiation time. And the final percentage consumption of Ami-6 reached about 23%, which is a little lower than that of Ami-2, as shown in Fig. 5d. The obvious intensity decrement in UV-vis absorption spectra and the calculated percentage consumption of ketones would provide a convincing evidence for the strong interaction between ketone and amine, and a reduction mechanism was already proposed by our group.^{31,32} Besides, both Ami-2 and Ami-6 have the same peripheral substituting tertiary amine group, thus their photolysis characterization alone in the absence of EDB was illustrated in Fig. S7. Very interestingly, similar photolysis upon LED@405 nm irradiation and chromophores consumptions were observed for these two ketones, respectively. This unique phenomenon could possibly be explained by the reaction of the amine moiety of one ketone molecule with the ketone moiety of another molecule, revealing the mono-component Type II photoinitiator behavior of the ketone derivatives presented in this work.

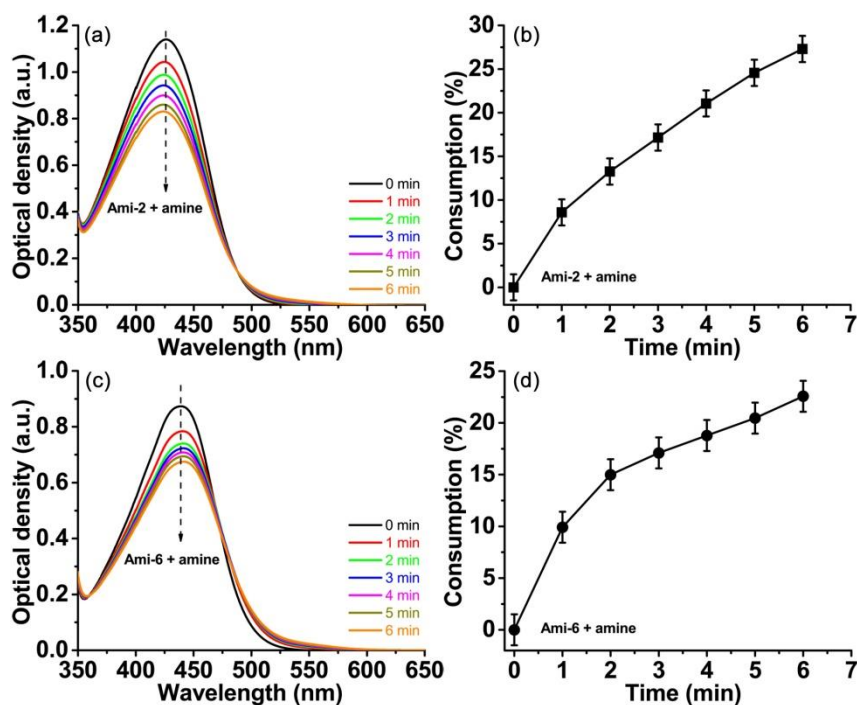


Fig. 5 Left: UV-vis absorption spectra of (a) Ami-2 (2.64×10^{-5} M) and (c) Ami-6 (2.21×10^{-5} M) in the presence of amine (EDB, 1.03×10^{-2} M) in the solvent of acetonitrile upon exposure to LED@405 nm irradiation for 6 min. Right: Consumption of ketones vs. LED@405 nm irradiation time for (b) Ami-2/amine and (d) Ami-6/amine system, respectively.

The steady state photolysis experiments of Ami-2 and Ami-6 in the presence of iodonium salt were also performed and studied, and the same LED with maximum emission wavelength at 405 nm was utilized as the irradiation source. The UV-vis absorption spectral changes of Ami-2 and Ami-6 in combination with iodonium salt upon the LED irradiation are presented in Fig. 6. Before irradiation, in combination with the iodonium salt (Iod; Speedcure 938), Ami-2 would show a maximum absorbance at 430 nm and Ami-6 would show a maximum absorbance at 440 nm, both illustrating a little bathochromic-shift when compared with that in combination with the amine (426 nm and 438 nm, respectively). Then, upon the LED@405 nm irradiation, a dramatic intensity decrement could be observed for Ami-2/Iod and Ami-6/Iod two-component systems (Fig. 6a, 6c). Interestingly, a distinct intensity increment could also be observed in the range between 500-600 nm in the UV-vis absorption spectra of Ami-6. It's believed that a strong oxidation interaction is formed between the ketone and the iodonium salt.^{31,32} Based on the decrement of the maximum absorbance in the UV-vis absorption spectra, the percentage consumption of ketones with the iodonium salt against LED irradiation time was also calculated. Remarkably, the photolysis of Ami-2 and Ami-6 in combination with iodonium salt is much faster than that in combination with amine upon the same LED irradiation. As shown in Fig. 6b, a nonlinear function was also depicted between the percentage consumption of Ami-2 and the LED irradiation time. And the final percentage consumption of Ami-2 within 60 s irradiation was about 56%, which is much higher than that with amine (27%). The percentage

consumption of Ami-6 against the LED irradiation time, in combination with iodonium salt, was shown in Fig. 6d. After irradiation for 60 s, the final percentage consumption of Ami-6 reached over 50%, which is also much higher than that with amine (23%). All the above presented steady state photolysis characterizations for Ami-2 and Ami-6 demonstrated high photoreactivity for the ketone/amine and ketone/Iod systems, revealing an excellent agreement with the high FCs and high polymerization rates for the free radical polymerization of TA. And for the ketone/amine/Iod three-component photoinitiating system, an oxidation-reduction reaction mechanism could be proposed upon visible LED irradiation.

Moreover, this photolysis characterization would be useful to explain the distinct photoinitiating abilities of the ketone derivatives containing the same central cyclohexanone core but different peripheral substituting groups. For example, Ami-2 and Ami-6 shared the same cyclohexanone cores with Anth-2 and Anth-6, respectively, but different peripheral substituting groups: tertiary amine or anthracene. However, the photoinitiating abilities of Ami-2 and Ami-6 based three-component systems for the free radical polymerization of acrylates are much better than those of Anth-2 and Anth-6 based systems, especially in the thick films. Further photolysis characterization revealed that upon the same LED irradiation, only a very tiny percent amount of Anth-2 and Anth-6 were consumed under the same condition with EDB or iodonium salt, as illustrated in Fig. S8.

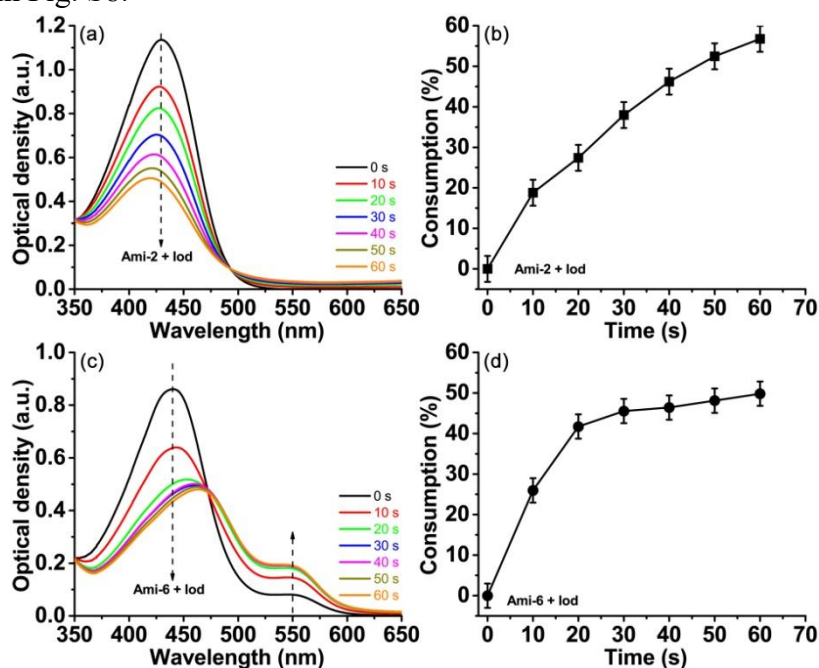


Fig. 6 Left: UV-vis absorption spectra of (a) Ami-2 (2.64×10^{-5} M) and (c) Ami-6 (2.21×10^{-5} M) in the presence of iodonium salt (Speedcure 938, 1.03×10^{-2} M) in the solvent of acetonitrile upon exposure to LED@405 nm irradiation for 60 s. Right: Consumption of ketones vs. LED@405 nm irradiation time for (b) Ami-2/Iod and (d) Ami-6/Iod system, respectively.

3.4. Excited state reactivity

According to the above steady state photolysis results, it seems that the ketones are

more reactive in combination with an iodonium salt than with an amine. Therefore, the excited state reactivity of ketones with the iodonium salt was characterized using a spectrofluorimeter. Fluorescence and fluorescence quenching experiments in acetonitrile are shown in Fig. 7 for the Ami-2/Iod and Ami-6/Iod two-component systems, respectively. Before the addition of the iodonium salt (Speedcure 938), both Ami-2 and Ami-6 could exhibit a strong emission in the range between 450 nm and 700 nm, and the fluorescence peak appeared at 558 nm for Ami-2 and at 556 nm for Ami-6, respectively. Then along with the increasing addition of iodonium salt from 0 M to $\sim 3.3 \times 10^{-3}$ M, an obvious and significant emission decline could be observed for these two ketones, indicating a clear fluorescence quenching phenomenon (Fig. 7a, 7c). Besides, through the Stern–Volmer treatment, a linear relationship between the fluorescence quenching of ketones and the concentration of added iodonium salt could be established, as shown in Fig. 7b and Fig. 7d.³³ All these results suggested that the iodonium salt would be a good fluorescence quencher for ketone derivatives and highlighted the strong interaction for the ketone/Iod system.

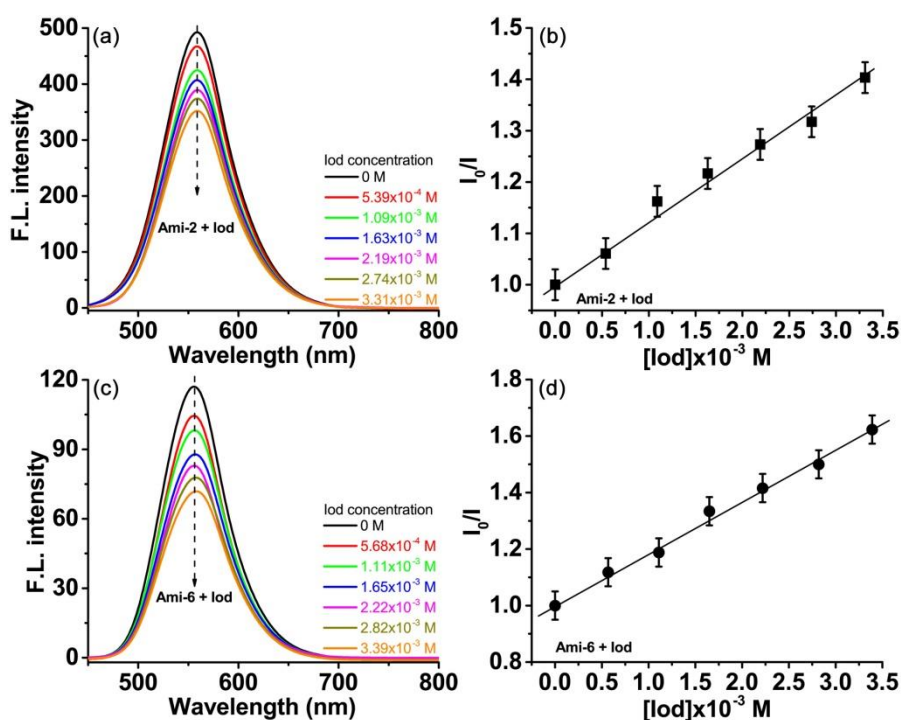


Fig. 7 Left: Fluorescence quenching of (a) Ami-2 (2.64×10^{-5} M) and (c) Ami-6 (2.21×10^{-5} M) upon the increasing addition of iodonium salt (Speedcure 938) in acetonitrile as the solvent, $\lambda_{exc}=420$ nm. Right: Stern–Volmer treatment for (b) Ami-2/Iod and (d) Ami-6/Iod fluorescence quenching, respectively.

3.5. Laser writing experiments using ketones-based photoinitiating systems

Remarkable initiating ability of the ketone derivatives based photoinitiating systems for the free radical polymerization of acrylates could also be reflected in spatially controlled photocuring 3D printing results. Some laser writing experiments upon a laser diode irradiation at 405 nm were successfully carried out under air using Ami-2/amine/Iod and Ami-6/amine/Iod three-component systems, respectively. The high

photosensitivity of these two photoinitiating systems could allow a highly efficient photocuring process in the irradiated area by the laser within a very short writing time (fewer than 3 min). Initiated by the Ami-2 and Ami-6 based photoinitiating systems, a tridimensional letter pattern, “CSC”, was fabricated from TA. Further profilometric observation of these patterns through a numerical optical microscope revealed excellent spatial resolution and really three-dimensional structure, as illustrated in Fig. 8. Remarkably, for the laser writing with Ami-2/amine/Iod system, the produced pattern was nearly 2 mm in thickness. However, under the same laser writing condition, the produced pattern with the Ami-6/amine/Iod system was thinner than 1 mm. This different depth of curing through laser writing experiments is just in accordance with the different photoinitiating abilities of the ketones-based initiating systems, considering that the Ami-2/amine/Iod system could induce the highest FC value of acrylates in thick films condition. Therefore, the 3D printing results from TA bring out a good example to demonstrate the high initiating ability of the three-component photoinitiating systems based on ketones.

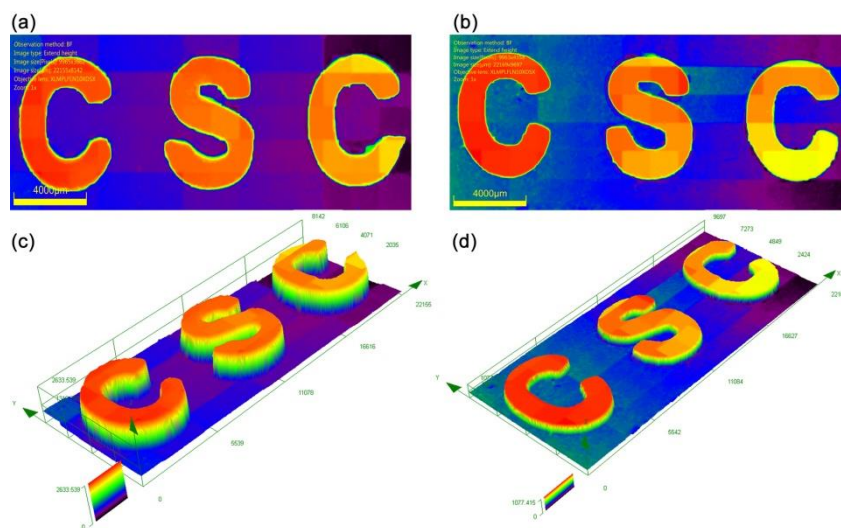


Fig. 8 Free radical photopolymerization for laser writing experiments of TA upon exposure to a laser diode@405 nm initiated by ketones-based three-component photoinitiating systems. Characterization of the generated patterns by numerical optical microscopy: (up) top surface morphology and (down) 3-D overall appearance in color pattern; (a), (c) for Ami-2/amine/Iod and (b), (d) for Ami-6/amine/Iod, respectively. The scale bar is 4000 μm .

4. Conclusion

In summary, twelve new ketone derivatives were introduced in this work as photoinitiators for the first time. And ketone/amine/Iod three-component photoinitiating systems were formed to initiate the photopolymerization of TA, a tetrafunctional polyether acrylate, upon LED@405 nm irradiation. The different photoinitiating abilities of the ketones-based photoinitiating systems for the free radical polymerization of acrylates were studied through RT-FTIR characterization. Among all these ketones, Ami-2 based photoinitiating system could induce the highest FC of acrylates in thick films, while Ami-6 based photoinitiating system could lead to the highest FC of acrylates in thin films. The high photoreactivity of Ami-2 and Ami-6 with amine (EDB) and iodonium salt (Iod; Speedcure 938) was thoroughly investigated by

the steady state photolysis and excited state fluorescence quenching experiments. Further the high photoinitiating ability of Ami-2/amine/Iod and Ami-6/amine/Iod three-component systems could also be reflected in the 3D printing application, and macroscopic 3D patterns were produced with excellent spatial resolution. This work not only provided novel ketone derivatives for the free radical polymerization of acrylates under mild conditions, but also expanded the application in photocuring 3D printing area. Further development of other high-performance ketone derivatives is under way and will be presented in the forthcoming papers.

Acknowledgments: This research is funded by the Region Grand Est for the grant “MIPPI-4D”. Yangyang Xu thanks the financial support from the Anhui Provincial Natural Science Foundation (1808085QB42), Natural Science Fund of Education Department of Anhui Province (KJ2018A0307), and China Scholarship Council (CSC). Pu Xiao acknowledges funding from the Australian Research Council (FT170100301). Computations were partly achieved using high performance computing (HPC) resources from the Meso centre of the University of Strasbourg. **The Agence Nationale de la Recherche (ANR agency) is acknowledged for its financial support through the PhD grant of Guillaume Noirbent (ANR-17-CE08-0054 VISICAT project. The Direction Générale de l’Armement (DGA)/Agence Innovation Defense (AID) is acknowledged for its financial support through the PhD grant of Damien Brunel.**

References

1. F. Dumur, *Eur. Polym. J.*, 2020, **126**, 109564.
2. H. Pan, S. Chen, M. Jin, J.-P. Malval, D. Wan and F. Morlet-Savary, *Polym. Chem.*, 2019, **10**, 1599–1609.
3. J. Yu, Y. Gao, S. Jiang and F. Sun, *Macromolecules*, 2019, **52**, 1707–1717.
4. J. Li, Y. Hao, M. Zhong, L. Tang, J. Nie and X. Zhu, *Dyes Pigments*, 2019, **165**, 467–473.
5. J. Li, X. Zhang, S. Ali, M. Y. Akram, J. Nie and X. Zhu, *J. Photoch. Photobio. A*, 2019, **384**, 112037.
6. F. Jasinski, P. B. Zetterlund, A. M. Braun and A. Chemtob, *Prog. Polym. Sci.*, 2018, **84**, 47–88.
7. S. Kasisomayajula, N. Jadhav and V. J. Gelling, *Prog. Org. Coat.*, 2016, **101**, 440–454.
8. A. Chemtob, N. Feillée, C. Ley, A. Ponche, S. Rigolet, C. Soraru, L. Ploux and D. L. Nouen, *Prog. Org. Coat.*, 2018, **121**, 80–88.
9. K. B. Riad, A. A. Arnold, J. P. Claverie, S. V. Hoa and P. M. Wood-Adams, *ACS Appl. Nano Mater.*, 2020, **3**, 2875–2880.
10. Z. Zhao, J. Wu, X. Mu, H. Chen, H. J. Qi and D. Fang, *Sci. Adv.*, 2017, **3**, e1602326.
11. J.-T. Lin, D.-C. Cheng, K.-T. Chen, Y.-C. Chiu and H.-W. Liu, *J. Polym. Sci.*, 2020, **58**, 683–691.
12. R. Anastasio, W. Peerbooms, R. Cardinaels and L. C. A. van Breemen, *Macromolecules*, 2019, **52**, 9220–9231.
13. W. Qiu, M. Li, Y. Yang, Z. Li and K. Dietliker, *Polym. Chem.*, 2020, **11**, 1356–1363.
14. Y.-H. Li and Y.-C. Chen, *Polym. Chem.*, 2020, **11**, 1504–1513.

15. S. Chen, M. Jin, J.-P. Malval, J. Fu, F. Morlet-Savary, H. Pan and D. Wan, *Polym. Chem.*, 2019, **10**, 6609–6621.
16. E. Hola, M. Pilch, M. Galek and J. Ortyl, *Polym. Chem.*, 2020, **11**, 480–495.
17. P. Sautrot-Ba, S. Jockusch, J.-P. Malval, V. Brezová, M. Rivard, S. Abbad-Andaloussi, A. Blacha-Grzechnik and D.-L. Versace, *Macromolecules*, 2020, **53**, 1129–1141.
18. L. Breloy, V. Brezová, A. Blacha-Grzechnik, M. Pisset, M. S. Yildirim, I. Yilmaz, Y. Yagci and D.-L. Versace, *Macromolecules*, 2020, **53**, 112–124.
19. J. Zhang, S. Wang, J. Lalevée, F. Morlet-Savary, E. S.-H. Lam, B. Graff, J. Liu, F. Xing and P. Xiao, *J. Polym. Sci.*, 2020, **58**, 792–802.
20. G. Ding, C. Jing, X. Qin, Y. Gong, X. Zhang, S. Zhang, Z. Luo, H. Li and F. Gao, *Dyes Pigments*, 2017, **137**, 456–467.
21. Y. Y. Xu, C. Jambou, K. Sun, J. Lalevée, A. Simon-Masseron and P. Xiao, *ACS Appl. Polym. Mater.*, 2019, **1**, 2854–2861.
22. Y.-Y. Xu, Z.-F. Ding, F.-Y. Liu, K. Sun, C. Dietlin, J. Lalevée and P. Xiao, *ACS Appl. Mater. Interfaces*, 2020, **12**, 1658–1664.
23. J. Zhang, N. Zivic, F. Dumur, P. Xiao, B. Graff, J. P. Fouassier, D. Gigmes and J. Lalevée, *Polym. Chem.*, 2018, **9**, 994–1003.
24. H. Mokbel, F. Dumur, C. R. Mayer, F. Morlet-Savary, B. Graff, D. Gigmes, J. Toufaily, T. Hamieh, J.-P. Fouassier and J. Lalevée, *Dyes Pigments*, 2014, **105**, 121–129.
25. P. Xiao, W. Hong, Y. Li, F. Dumur, B. Graff, J. P. Fouassier, D. Gigmes and J. Lalevée, *Polym. Chem.*, 2014, **5**, 2293–2300.
26. C. Pigot, G. Noirbent, S. Peralta, S. Duval, T.-T. Bui, P.-H. Aubert, M. Nechab, D. Gigmes and F. Dumur, *Dyes Pigments*, 2020, **175**, 108182.
27. L. G. Possato, E. Pereira, R. G.L. Goncalves, S. H. Pulcinelli, L. Martins and C. V. Santilli, *Catal. Today*, 2020, **344**, 52–58.
28. J. Chen, Y. Li, Z. Xiao, H. He and S. Gao, *Org. Lett.*, 2020, **22**, 1485–1489.
29. E. Hola, J. Ortyl, M. Jankowska, M. Pilch, M. Galek, F. Morlet-Savary, B. Graff, C. Dietlin and J. Lalevée, *Polym. Chem.*, 2020, **11**, 922–935.
30. J. Zhang, F. Dumur, P. Xiao, B. Graff, D. Bardelang, D. Gigmes, J. P. Fouassier and J. Lalevée, *Macromolecules*, 2015, **48**, 2054–2063.
31. K. Sun, Y. Xu, F. Dumur, F. Morlet-Savary, H. Chen, C. Dietlin, B. Graff, J. Lalevée and P. Xiao, *Polym. Chem.*, 2020, **11**, 2230–2242.
32. Y. Xu, G. Noirbent, D. Brunel, F. Liu, D. Gigmes, K. Sun, Y. Zhang, S. Liu, F. Morlet-Savary, P. Xiao, F. Dumur and J. Lalevée. *Eur. Polym. J.*, 2020, **132**, 109737.
33. A. A. Mousawi, D. M. Lara, G. Noirbent, F. Dumur, J. Toufaily, T. Hamieh, T.-T. Bui, F. Goubard, B. Graff, D. Gigmes, J. P. Fouassier and J. Lalevée, *Macromolecules*, 2017, **50**, 4913–4926.

Supporting information

Novel ketone derivatives based photoinitiating systems for free radical polymerization under mild conditions and 3D printing

Yangyang Xu,^{a,b*} Guillaume Noirbent,^c Damien Brunel,^c Zhaofu Ding,^a Didier Gimes,^c Yijun Zhang,^b Shaohui Liu,^b Bernadette Graff,^b Pu Xiao,^{d*} Frédéric Dumur^{c*} and Jacques Lalevée^{b*}

^aCollege of Chemistry and Materials Science, Anhui Normal University, South Jiuhua Road 189, Wuhu 241002, P. R. China. E-mail: ahnuxyy@ahnu.edu.cn

^bInstitut de Science des Matériaux de Mulhouse, IS2M-UMR CNRS 7361, UHA, 15, rue Jean Starcky, Cedex 68057 Mulhouse, France. E-mail: jacques.lalevee@uha.fr

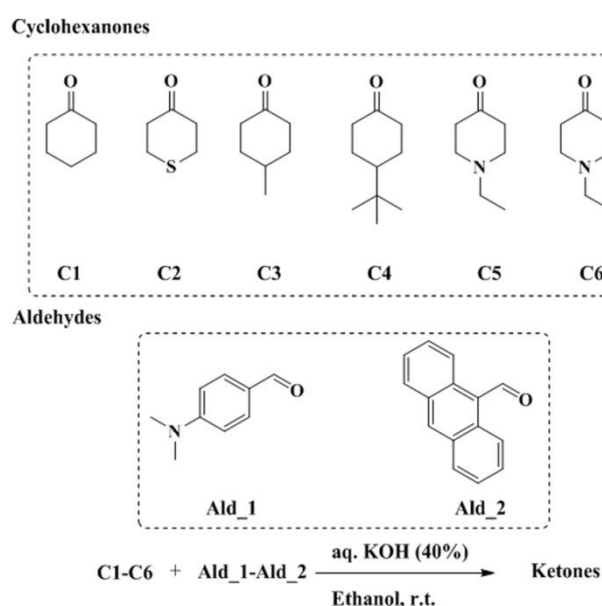
^cAix Marseille Univ, CNRS, ICR UMR 7273, F-13397 Marseille, France. E-mail: Frederic.dumur@univ-amu.fr

^dResearch School of Chemistry, Australian National University, Canberra, ACT 2601, Australia. E-mail: pu.xiao@anu.edu.au

Index

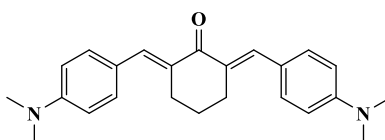
1. Chemical synthesis.
2. Formulation preparation.
3. UV-vis absorption property.
4. Theoretical computation.
5. Photopolymerization.
6. Steady state photolysis.

All reagents and solvents were purchased from Aldrich or Alfa Aesar and used as received without further purification. Mass spectroscopy was performed by the Spectropole of Aix-Marseille University. ESI mass spectral analyses were recorded with a 3200 QTRAP (Applied Biosystems SCIEX) mass spectrometer. The HRMS mass spectral analysis was performed with a QStar Elite (Applied Biosystems SCIEX) mass spectrometer. Elemental analyses were recorded with a Thermo Finnigan EA 1112 elemental analysis apparatus driven by the Eager 300 software. ^1H and ^{13}C NMR spectra were determined at room temperature in 5 mm o.d. tubes on a Bruker Avance 400 spectrometer of the Spectropole: ^1H (400 MHz) and ^{13}C (100 MHz). The ^1H chemical shifts were referenced to the solvent peaks: DMSO (2.49 ppm), CDCl_3 (7.26 ppm) and the ^{13}C chemical shifts were referenced to the solvent peaks: DMSO (49.5 ppm), CDCl_3 (77.0 ppm), respectively. All photoinitiators were prepared with analytical purity up to accepted standards for new organic compounds (>98%), which were checked by high field NMR analysis.



Scheme S1 Chemical synthesis for the twelve ketones.

Synthesis of 2,6-bis((*E*)-4-(dimethylamino)benzylidene)cyclohexan-1-one (Ami-1)

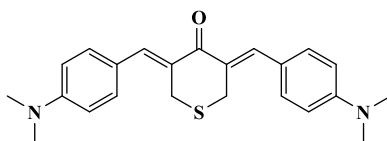


Chemical Formula: $\text{C}_{24}\text{H}_{28}\text{N}_2\text{O}$
Molecular Weight: 360.5010

Cyclohexanone (0.98 g, 10 mmol, $M = 98.14$ g/mol) and 4-dimethylaminobenzaldehyde (2.98 g, 20 mmol, $M = 149.19$ g/mol) were dissolved in ethanol (50 mL) and aq. KOH (40%) (15 mL) was added. The solution was stirred at room temperature overnight. During reaction, a precipitate formed. It was filtered off,

washed several times with ethanol and dried under vacuum. The resulting solid was dissolved in dichloromethane and the solution was filtered on a plug of SiO₂ using dichloromethane as the eluent. The solvent was removed under reduced pressure. Dissolution in a minimum of dichloromethane followed by addition of pentane precipitated a solid that was filtered off, washed several times with pentane and dried under vacuum (3.12 g, 87% yield). ¹H NMR (CDCl₃) δ: 1.77-1.85 (m, 2H), 2.91-2.96 (m, 4H), 3.02 (s, 12H), 6.72 (d, 4H, J = 8.7 Hz), 7.44 (d, 4H, J = 8.7 Hz), 7.76 (s, 2H); ¹³C NMR (CDCl₃) δ: 23.2, 28.7, 40.2, 111.7, 124.4, 132.4, 132.5, 137.0, 150.3, 190.1; HRMS (ESI MS) m/z: theor: 360.2202 found: 360.2203 (M⁺ detected).

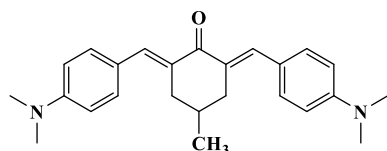
Synthesis of 3,5-bis((Z)-4-(dimethylamino)benzylidene)tetrahydro-4H-thiopyran-4-one (Ami-2)



Chemical Formula: C₂₃H₂₆N₂OS
Molecular Weight: 378.5340

Tetrahydro-4H-thiopyran-4-one (1.17 g, 10 mmol, M = 116.18 g/mol) and 4-dimethylaminobenzaldehyde (2.98 g, 20 mmol, M = 149.19 g/mol) were dissolved in ethanol (50 mL) and aq. KOH (40%) (15 mL) was added. The solution was stirred at room temperature overnight. During reaction, a precipitate formed. It was filtered off, washed several times with ethanol and dried under vacuum. The resulting solid was dissolved in dichloromethane and the solution was filtered on a plug of SiO₂ using dichloromethane as the eluent. The solvent was removed under reduced pressure. Dissolution in a minimum of dichloromethane followed by addition of pentane precipitated a solid that was filtered off, washed several times with pentane and dried under vacuum (3.44 g, 91% yield). ¹H NMR (CDCl₃) δ: 3.03 (s, 12H), 3.97 (s, 4H), 6.72 (d, 4H, J = 8.8 Hz), 7.37 (d, 4H, J = 8.8 Hz), 7.75 (s, 2H); ¹³C NMR (CDCl₃) δ: 30.4, 40.2, 111.9, 130.1, 132.3, 137.2, 150.5, 188.6; HRMS (ESI MS) m/z: theor: 378.1766 found: 378.1764 (M⁺ detected).

Synthesis of 2,6-bis((E)-4-(dimethylamino)benzylidene)-4-methylcyclohexan-1-one (Ami-3)

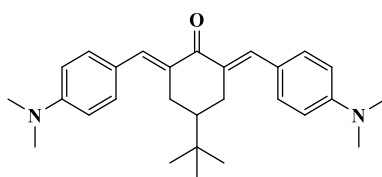


Chemical Formula: C₂₅H₃₀N₂O
Molecular Weight: 374.5280

4-Methylcyclohexan-1-one (1.12 g, 10 mmol, M = 112.17 g/mol) and 4-dimethylaminobenzaldehyde (2.98 g, 20 mmol, M = 149.19 g/mol) were dissolved in ethanol (50 mL) and aq. KOH (40%) (15 mL) was added. The solution was stirred at room temperature overnight. During reaction, a precipitate formed. It was filtered off, washed several times with ethanol and dried under vacuum. The resulting solid was

dissolved in dichloromethane and the solution was filtered on a plug of SiO₂ using dichloromethane as the eluent. The solvent was removed under reduced pressure. Dissolution in a minimum of dichloromethane followed by addition of pentane precipitated a solid that was filtered off, washed several times with pentane and dried under vacuum (3.07 g, 82% yield). ¹H NMR (CDCl₃) δ: 1.10 (d, 3H, J = 6.5 Hz), 1.85-1.93 (m, 1H), 2.46-2.54 (m, 2H), 3.02 (s, 12H), 3.07-3.19 (m, 2H), 6.73 (d, 4H, J = 8.6 Hz), 7.45 (d, 4H, J = 8.6 Hz), 7.76 (s, 2H); ¹³C NMR (CDCl₃) δ: 21.9, 29.5, 36.9, 40.2, 111.7, 124.3, 131.7, 132.4, 137.2, 150.4, 189.8; HRMS (ESI MS) m/z: theor: 374.2358 found: 374.2354 (M⁺ detected).

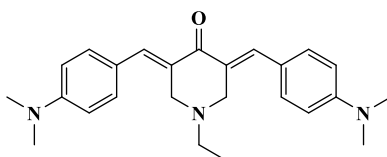
Synthesis of 4-(*tert*-butyl)-2,6-bis((*E*)-4-(dimethylamino)benzylidene)cyclohexan-1-one (Ami-4)



Chemical Formula: C₂₈H₃₆N₂O
Molecular Weight: 416.6090

4-(*Tert*-butyl)cyclohexan-1-one (1.54 g, 10 mmol, M = 154.25 g/mol) and 4-dimethylaminobenzaldehyde (2.98 g, 20 mmol, M = 149.19 g/mol) were dissolved in ethanol (50 mL) and aq. KOH (40%) (15 mL) was added. The solution was stirred at room temperature overnight. During reaction, a precipitate formed. It was filtered off, washed several times with ethanol and dried under vacuum. The resulting solid was dissolved in dichloromethane and the solution was filtered on a plug of SiO₂ using dichloromethane as the eluent. The solvent was removed under reduced pressure. Dissolution in a minimum of dichloromethane followed by addition of pentane precipitated a solid that was filtered off, washed several times with pentane and dried under vacuum (3.46 g, 83% yield). ¹H NMR (CDCl₃) δ: 1.00 (s, 9H), 1.47-1.56 (m, 1H), 2.42-2.48 (m, 2H), 3.03 (s, 12H), 3.16-3.20 (m, 2H), 6.75 (d, 4H, J = 8.3 Hz), 7.45 (d, 4H, J = 8.3 Hz), 7.73 (d, 2H, J = 2.2 Hz); ¹³C NMR (CDCl₃) δ: 27.5, 29.7, 32.5, 40.2, 44.4, 111.8, 132.4, 136.9, 150.3, 190.2; HRMS (ESI MS) m/z: theor: 416.2828 found: 416.2828 (M⁺ detected).

Synthesis of 3,5-bis((*E*)-4-(dimethylamino)benzylidene)-1-ethylpiperidin-4-one (Ami-5)

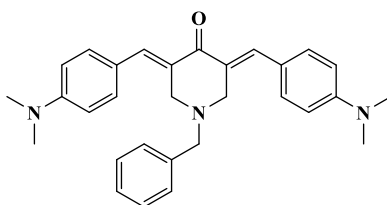


Chemical Formula: C₂₅H₃₁N₃O
Molecular Weight: 389.5430

1-Ethylpiperidin-4-one (1.27 g, 10 mmol, M = 127.19 g/mol) and 4-dimethylaminobenzaldehyde (2.98 g, 20 mmol, M = 149.19 g/mol) were dissolved in ethanol (50 mL)

and aq. KOH (40%) (15 mL) was added. The solution was stirred at room temperature overnight. During reaction, a precipitate formed. It was filtered off, washed several times with ethanol and dried under vacuum. The resulting solid was dissolved in dichloromethane and the solution was filtered on a plug of SiO₂ using dichloromethane as the eluent. The solvent was removed under reduced pressure. Dissolution in a minimum of dichloromethane followed by addition of pentane precipitated a solid that was filtered off, washed several times with pentane and dried under vacuum (3.70 g, 95% yield). ¹H NMR (CDCl₃) δ: 1.03 (t, 3H, J = 7.1 Hz), 2.59 (q, 2H, J = 7.1 Hz), 2.95 (s, 12H), 3.81 (s, 4H), 6.64 (d, 4H, J = 8.9 Hz), 7.28 (d, 4H, J = 8.9 Hz), 7.71 (s, 2H); ¹³C NMR (CDCl₃) δ: 12.5, 40.1, 54.5, 111.7, 123.5, 132.5, 136.9, 150.6, 186.8; HRMS (ESI MS) m/z: theor: 389.2467 found: 389.2470 (M⁺ detected).

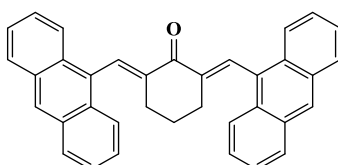
Synthesis of 1-benzyl-3,5-bis((E)-4-(dimethylamino)benzylidene)piperidin-4-one (Ami-6)



Chemical Formula: C₃₀H₃₃N₃O
Molecular Weight: 451.6140

1-Benzylpiperidin-4-one (1.90 g, 10 mmol, M = 189.26 g/mol) was dissolved in a mixture of ethanol (20 mL) and water (10 mL). 4-Dimethylaminobenzaldehyde (2.98 g, 20 mmol, M = 149.19 g/mol) and NaOH 1M (10 mL) were then added at 0°C. During stirring, a sticky solid formed so that THF (20-30 mL) was added to maintain the stirring of the solution. The solution was stirred at room temperature overnight. The yellow precipitate was filtrated off, washed with ethanol and dried under vacuum (3.83 g, 85% yield). ¹H NMR (CDCl₃) δ: 3.01 (s, 12H), 3.72-3.77 (m, 2H), 3.91 (brs, 4H), 6.68 (d, 4H, J = 8.9 Hz), 7.19-7.32 (m, 9H), 7.77 (brs, 2H); ¹H NMR (DMSO-d₆) δ: 2.98 (s, 12H), 3.75 (s, 2H), 3.79 (s, 4H), 6.74 (d, 4H, J = 8.9 Hz), 7.19-7.23 (m, 1H), 7.27-7.33 (m, 8H), 7.50 (s, 2H); ¹³C NMR (DMSO-d₆) δ: 25.1, 54.6, 67.0, 111.8, 122.2, 127.1, 128.2, 128.8, 129.1, 132.3, 134.9, 138.0, 150.6, 185.7; HRMS (ESI MS) m/z: theor: 451.2624 found: 451.2626 (M⁺ detected).

Synthesis of 2,6-bis(anthracen-9-ylmethylene)cyclohexan-1-one (Anth-1)

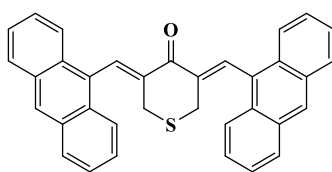


Chemical Formula: C₃₆H₂₆O
Molecular Weight: 474.6030

Cyclohexanone (0.98 g, 10 mmol, M = 98.14 g/mol) and anthracene-9-carbaldehyde (4.12 g, 20 mmol, M = 206.24 g/mol) were dissolved in ethanol (50 mL) and aq. KOH (40%) (15 mL) was added. The solution was stirred at room temperature overnight.

During reaction, a precipitate formed. It was filtered off, washed several times with ethanol and dried under vacuum. The resulting solid was dissolved in dichloromethane and the solution was filtered on a plug of SiO₂ using dichloromethane as the eluent. The solvent was removed under reduced pressure. Dissolution in a minimum of dichloromethane followed by addition of pentane precipitated a solid that was filtered off, washed several times with pentane and dried under vacuum (3.74 g, 79% yield). ¹H NMR (CDCl₃) δ: 1.46-1.55 (m, 2H), 2.27-2.31 (m, 4H), 7.49-7.57 (m, 8H), 8.04-8.11 (m, 8H), 8.48 (s, 2H), 8.68 (s, 2H); ¹³C NMR (CDCl₃) δ: 22.5, 25.6, 28.6, 125.4, 125.9, 126.0, 127.4, 128.9, 129.1, 130.5, 131.3, 135.8, 140.9, 188.6; HRMS (ESI MS) m/z: theor: 474.1984 found: 474.1982 (M⁺ detected).

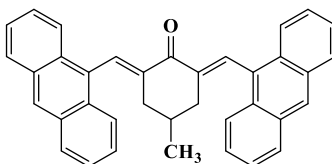
Synthesis of 3,5-bis(anthracen-9-ylmethylene)tetrahydro-4H-thiopyran-4-one (Anth-2)



Chemical Formula: C₃₅H₂₄OS
Molecular Weight: 492.6360

Tetrahydro-4H-thiopyran-4-one (1.17 g, 10 mmol, M = 116.18 g/mol) and anthracene-9-carbaldehyde (4.12 g, 20 mmol, M = 206.24 g/mol) were dissolved in ethanol (50 mL) and aq. KOH (40%) (15 mL) was added. The solution was stirred at room temperature overnight. During reaction, a precipitate formed. It was filtered off, washed several times with ethanol and dried under vacuum. The resulting solid was dissolved in dichloromethane and the solution was filtered on a plug of SiO₂ using dichloromethane as the eluent. The solvent was removed under reduced pressure. Dissolution in a minimum of dichloromethane followed by addition of pentane precipitated a solid that was filtered off, washed several times with pentane and dried under vacuum (4.04 g, 82% yield). ¹H NMR (CDCl₃) δ: 3.32 (s, 4H), 7.50-7.60 (m, 8H), 8.05-8.12 (m, 8H), 8.49 (s, 2H), 8.68 (s, 2H); ¹³C NMR (CDCl₃) δ: 30.7, 125.5, 125.6, 126.4, 127.9, 129.0, 129.16, 129.18, 131.3, 135.4, 138.2, 187.2; HRMS (ESI MS) m/z: theor: 492.1548 found: 492.1544 (M⁺ detected).

Synthesis of 2,6-bis(anthracen-9-ylmethylene)-4-methylcyclohexan-1-one (Anth-3)

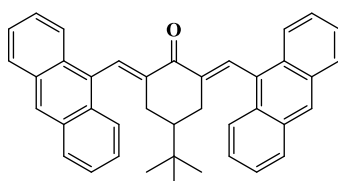


Chemical Formula: C₃₇H₂₈O
Molecular Weight: 488.6300

4-Methylcyclohexan-1-one (1.12 g, 10 mmol, M = 112.17 g/mol) and anthracene-9-carbaldehyde (4.12 g, 20 mmol, M = 206.24 g/mol) were dissolved in ethanol (50 mL) and aq. KOH (40%) (15 mL) was added. The solution was stirred at room temperature overnight. During reaction, a precipitate formed. It was filtered off, washed several

times with ethanol and dried under vacuum. The resulting solid was dissolved in dichloromethane and the solution was filtered on a plug of SiO₂ using dichloromethane as the eluent. The solvent was removed under reduced pressure. Dissolution in a minimum of dichloromethane followed by addition of pentane precipitated a solid that was filtered off, washed several times with pentane and dried under vacuum (4.15 g, 85% yield). ¹H NMR (CDCl₃) δ: 0.58 (d, 3H, J = 6.6 Hz), 1.74-1.81 (m, 1H), 2.01-2.08 (m, 2H), 2.28-2.32 (m, 2H), 7.50-7.56 (m, 8H), 8.04-8.13 (m, 8H), 8.48 (s, 2H), 8.68 (s, 2H); ¹³C NMR (CDCl₃) δ: 20.8, 28.8, 36.4, 125.39, 125.43, 125.7, 126.0, 127.3, 128.88, 128.92, 129.1, 129.2, 130.6, 131.2, 131.3, 136.2, 140.1, 188.3; HRMS (ESI MS) m/z: theor: 488.2140 found: 488.2142 (M⁺ detected).

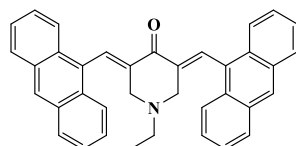
Synthesis of 2,6-bis(anthracen-9-ylmethylene)-4-(*tert*-butyl)cyclohexan-1-one (Anth-4)



Chemical Formula: C₄₀H₃₄O
Molecular Weight: 530.7110

4-(*Tert*-butyl)cyclohexan-1-one (1.54 g, 10 mmol, M = 154.25 g/mol) and anthracene-9-carbaldehyde (4.12 g, 20 mmol, M = 206.24 g/mol) were dissolved in ethanol (50 mL) and aq. KOH (40%) (15 mL) was added. The solution was stirred at room temperature overnight. During reaction, a precipitate formed. It was filtered off, washed several times with ethanol and dried under vacuum. The resulting solid was dissolved in dichloromethane and the solution was filtered on a plug of SiO₂ using dichloromethane as the eluent. The solvent was removed under reduced pressure. Dissolution in a minimum of dichloromethane followed by addition of pentane precipitated a solid that was filtered off, washed several times with pentane and dried under vacuum (4.72 g, 89% yield). ¹H NMR (CDCl₃) δ: 0.33 (s, 9H), 1.49-1.56 (m, 1H), 1.98-2.04 (m, 2H), 2.39-2.43 (m, 2H), 7.49-7.55 (m, 8H), 8.05-8.12 (m, 8H), 8.48 (s, 2H), 8.64 (d, 2H, J = 2.4 Hz); ¹³C NMR (CDCl₃) δ: 26.7, 29.6, 32.1, 44.0, 125.40, 125.41, 125.7, 125.9, 125.95, 126.01, 127.2, 130.5, 131.3, 135.8, 140.9, 188.8; HRMS (ESI MS) m/z: theor: 530.2610 found: 530.2611 (M⁺ detected).

Synthesis of 3,5-bis(anthracen-9-ylmethylene)-1-ethylpiperidin-4-one (Anth-5)

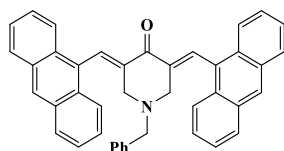


Chemical Formula: C₃₇H₂₉NO
Molecular Weight: 503.6450

1-Ethylpiperidin-4-one (1.27 g, 10 mmol, M = 127.19 g/mol) and anthracene-9-carbaldehyde (4.12 g, 20 mmol, M = 206.24 g/mol) and NaOH 1M (10 mL) were

dissolved in ethanol (50 mL) and aq. KOH (40%) (15 mL) was added. The solution was stirred at room temperature overnight. During reaction, a precipitate formed. It was filtered off, washed several times with ethanol and dried under vacuum. The resulting solid was dissolved in dichloromethane and the solution was filtered on a plug of SiO₂ using dichloromethane as the eluent. The solvent was removed under reduced pressure. Dissolution in a minimum of dichloromethane followed by addition of pentane precipitated a solid that was filtered off, washed several times with pentane and dried under vacuum (4.17 g, 83% yield). ¹H NMR (CDCl₃) δ: 0.49 (t, 3H, J = Hz), 2.17 (brs, 2H), 3.20 (brs, 4H), 7.50-7.57 (m, 8H), 8.04-8.11 (m, 8H), 8.49 (s, 2H), 8.74 (s, 2H); ¹³C NMR (CDCl₃) δ: 11.8, 50.5, 54.1, 68.0, 125.5, 125.7, 126.2, 127.7, 128.9, 129.0, 129.5, 135.5, 137.6, 185.9; HRMS (ESI MS) m/z: theor: 502.2297 found: 502.2298 (M⁺ detected).

Synthesis of 3,5-bis(anthracen-9-ylmethylene)-1-benzylpiperidin-4-one (Anth-6)



Chemical Formula: C₄₂H₃₁NO
Molecular Weight: 565.7160

1-Benzylpiperidin-4-one (1.90 g, 10 mmol, M = 189.26 g/mol) and anthracene-9-carbaldehyde (4.12 g, 20 mmol, M = 206.24 g/mol) were dissolved in ethanol (50 mL) and aq. KOH (40%) (15 mL) was added. The solution was stirred at room temperature overnight. During reaction, a precipitate formed. It was filtered off, washed several times with ethanol and dried under vacuum. The resulting solid was dissolved in dichloromethane and the solution was filtered on a plug of SiO₂ using dichloromethane as the eluent. The solvent was removed under reduced pressure. Dissolution in a minimum of dichloromethane followed by addition of pentane precipitated a solid that was filtered off, washed several times with pentane and dried under vacuum (4.97g, 88% yield). ¹H NMR (CDCl₃) δ: 3.18 (s, 2H), 3.23 (s, 4H), 6.68 (d, 4H, J = 3.8 Hz), 6.82-6.85 (m, 1H), 7.49-7.51 (m, 8H), 8.01-8.08 (m, 8H), 8.44 (s, 2H), 8.75 (s, 2H); ¹H NMR (DMSO-d₆) δ: 3.18 (s, 4H), 3.29 (s, 2H), 6.58 (t, 2H, J = 7.3 Hz), 6.64 (d, 2H, J = 6.9 Hz), 6.77 (t, 1H, J = 7.2 Hz), 7.57-7.64 (m, 8H), 8.07 (d, 4H, J = 8.3 Hz), 8.15 (d, 4H, J = 9.3 Hz), 8.58 (s, 2H), 8.69 (s, 2H); HRMS (ESI MS) m/z: theor: 564.2453 found: 564.2458 (M⁺ detected); Anal. Calc. for C₄₂H₃₁NO: C, 91.5; H, 5.7; O, 2.8; Found: C, 91.4; H, 5.2; O, 3.0 %.

Table S1. Basic formulation for the free radical photopolymerization.

Ketone (0.1%, w)	amine (EDB) (2%, w)	Iod (Speedcure 938) (2%, w)	TA (Ebecryl 40)
0.2 mg	40.0 mg	40.0 mg	2.0 g

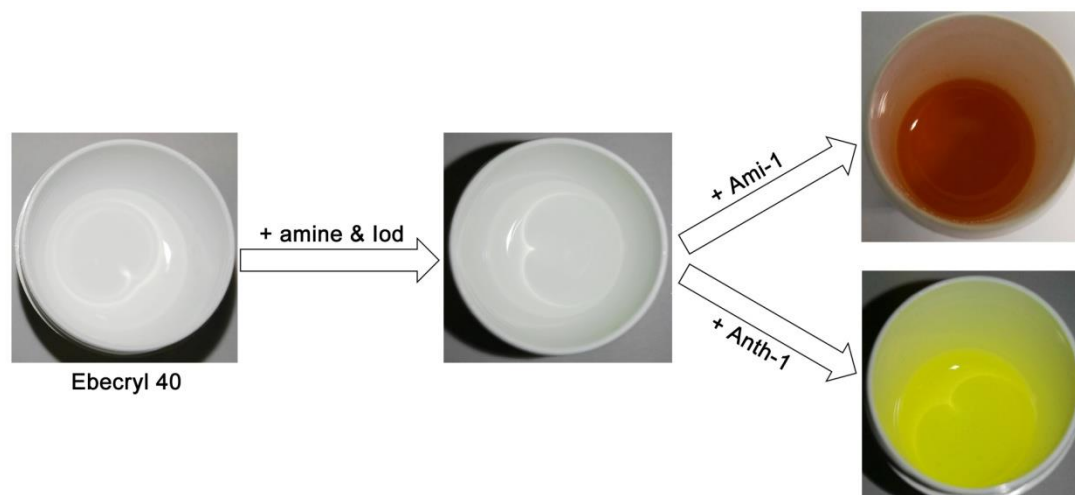


Figure S1 *In situ* photograph for the preparation of the LED sensitive formulation.

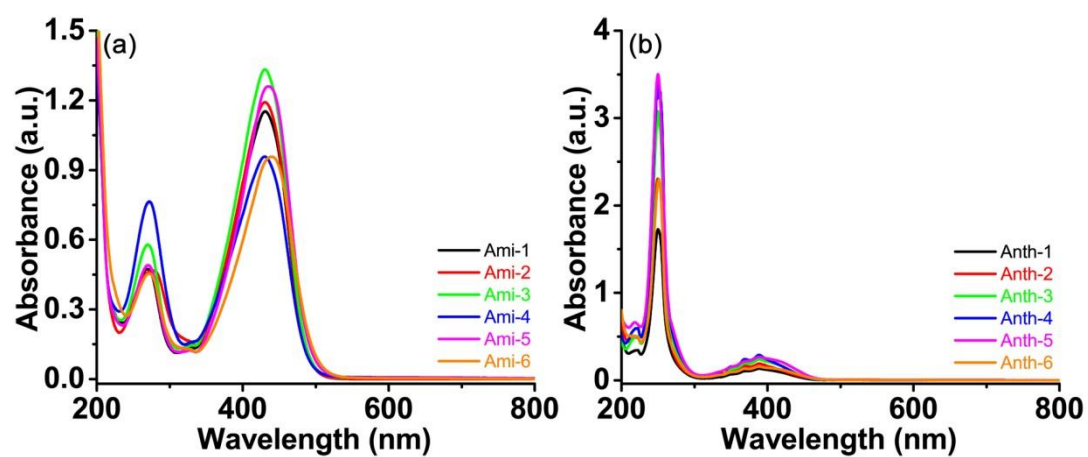
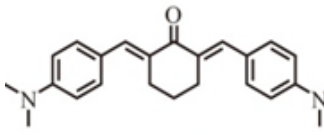
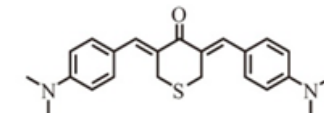
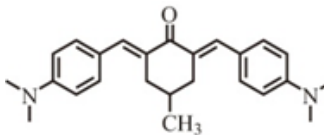
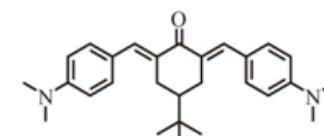
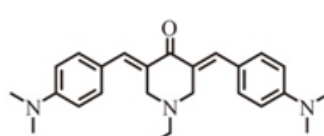
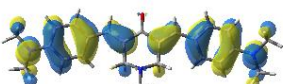
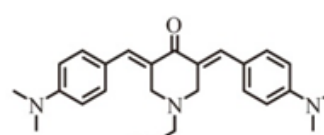
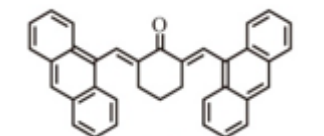


Figure S2 UV-vis absorption spectra of the twelve ketone derivatives dissolved in acetonitrile (0.01 mg/mL).

	HOMO	LUMO
<p>(Ami-1)</p> 		
<p>(Ami-2)</p> 		
<p>(Ami-3)</p> 		
<p>(Ami-4)</p> 		
<p>(Ami-5)</p> 		
<p>(Ami-6)</p> 		
<p>(Anth-1)</p> 		

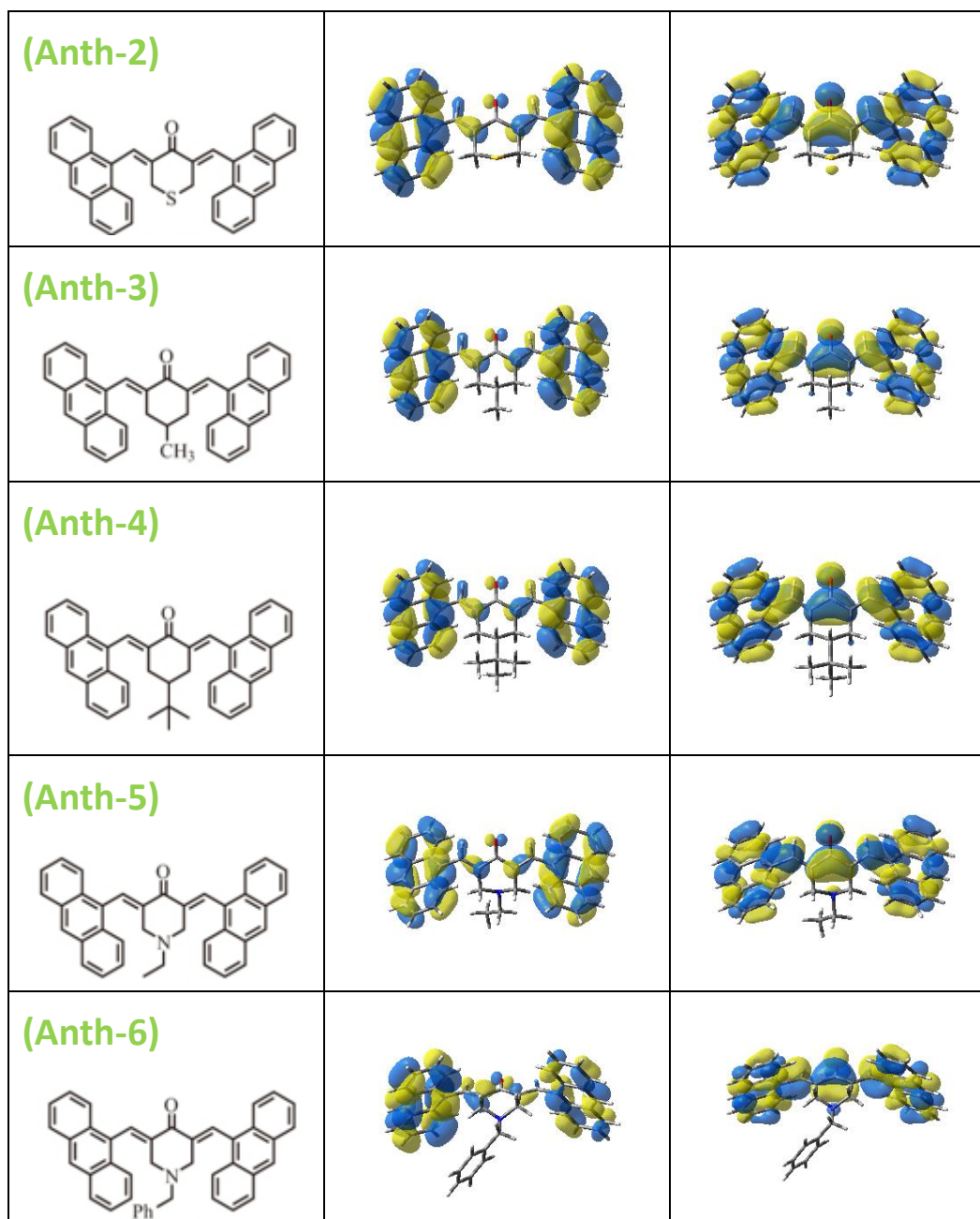


Figure S3 Frontier molecular orbitals properties (HOMOs and LUMOs) of newly proposed ketones (calculated at UB3LYP/6-31G* level – iso value=0.02).

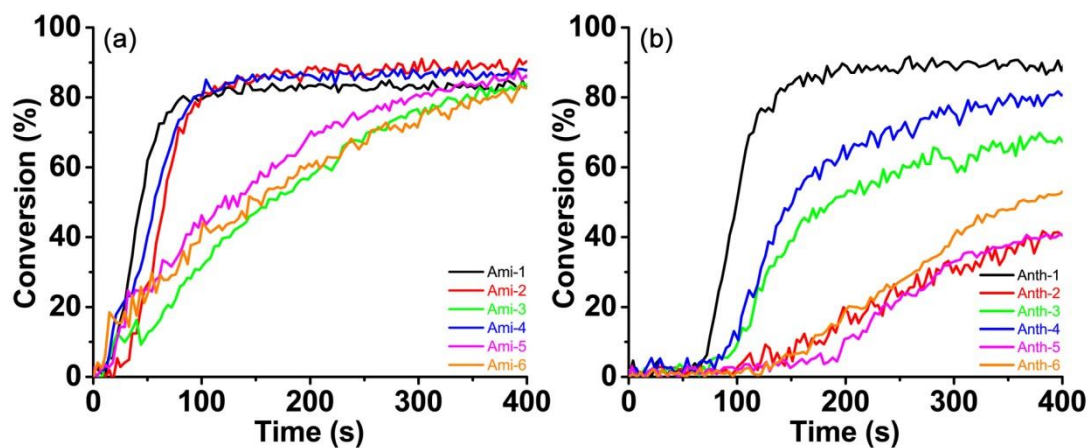


Figure S4 Photopolymerization profiles of TA (acrylate function conversion vs. irradiation time) in thick films (thickness \approx 1.4 mm) upon exposure to a LED@405 nm in the presence of ketone/amine/Iod (0.1%/2%/2%, w/w/w) three-component photoinitiating systems.

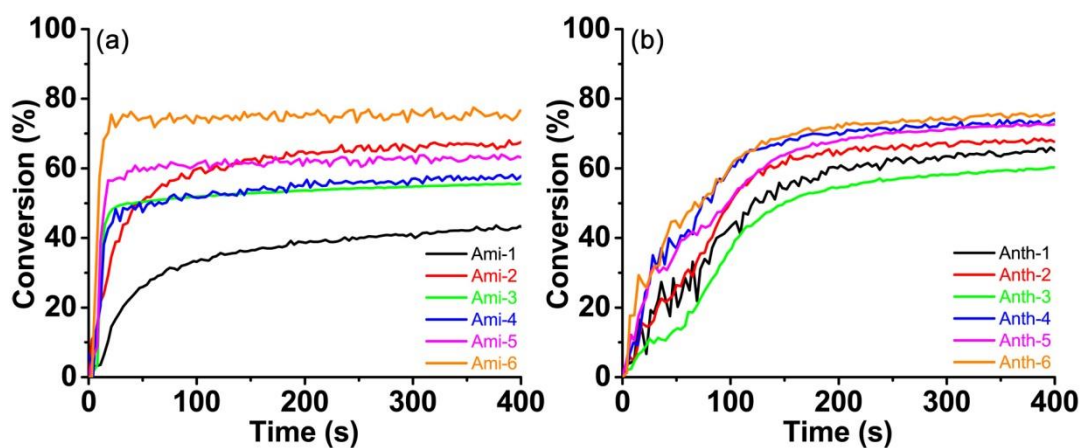


Figure S5 Photopolymerization profiles of TA (acrylate function conversion vs. irradiation time) in thin films (thickness \approx 25 μ m) upon exposure to a LED@405 nm in the presence of ketone/amine/Iod (0.1%/2%/2%, w/w/w) three-component photoinitiating systems.

Table S2 Curve slopes of the photopolymerization profiles for reactive acrylates in thick and thin films conditions, respectively, upon exposure to LED@405 nm for 400 s in the presence of ketone/amine/Iod (0.1%/2%/2%, w/w/w) three-component photoinitiating systems.

Slopes (s^{-1}) (in thick)	Ami-1	Ami-2	Ami-3	Ami-4	Ami-5	Ami-6
	~1.44	~1.36	~0.32	~1.39	~0.31	~0.28
	Anth-1	Anth-2	Anth-3	Anth-4	Anth-5	Anth-6
Slopes (s^{-1}) (in thin)	~1.32	~0.14	~0.31	~0.54	~0.23	~0.21
	Ami-1	Ami-2	Ami-3	Ami-4	Ami-5	Ami-6
	~0.45	~0.89	~2.47	~2.26	~3.47	~4.72
	Anth-1	Anth-2	Anth-3	Anth-4	Anth-5	Anth-6
	~0.38	~0.45	~0.38	~0.61	~0.44	~0.61

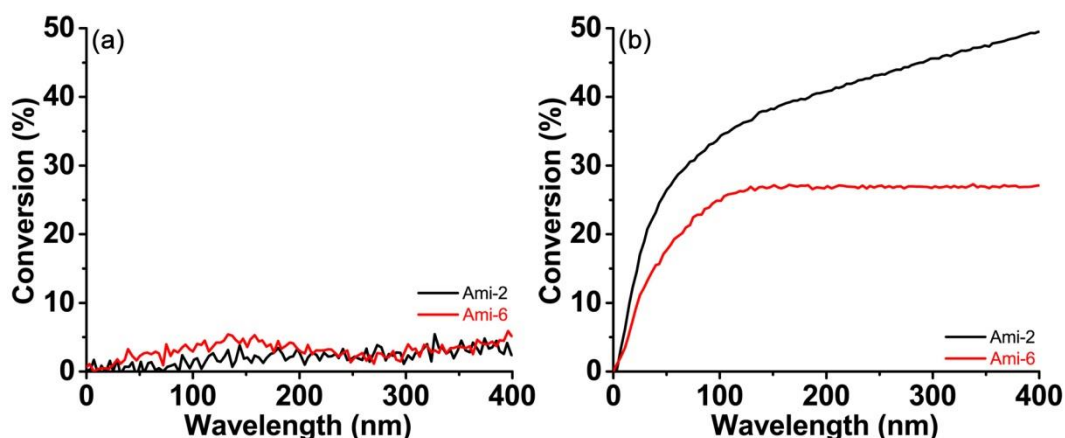


Figure S6 Photopolymerization profiles of TA (acrylate function conversion vs. irradiation time) initiated by Ami-2 or Ami-6 (0.1%, w) in the absence of any photo-additives (EDB or Speedcure 938) upon exposure to a LED@405 nm for 400 s: (a) in thick films (thickness ≈ 1.4 mm) and (b) in thin films (thickness ≈ 25 μ m), respectively.

Table S3 Final conversions (FCs) for reactive acrylates of TA in thick and thin films conditions, respectively, upon exposure to LED@405 nm for 400 s in the presence of ketones alone without any photo-additives.

FCs (in thick)	Ami-2	Ami-6
	3%	5%
FCs (in thin)	Ami-2	Ami-6
	49%	27%

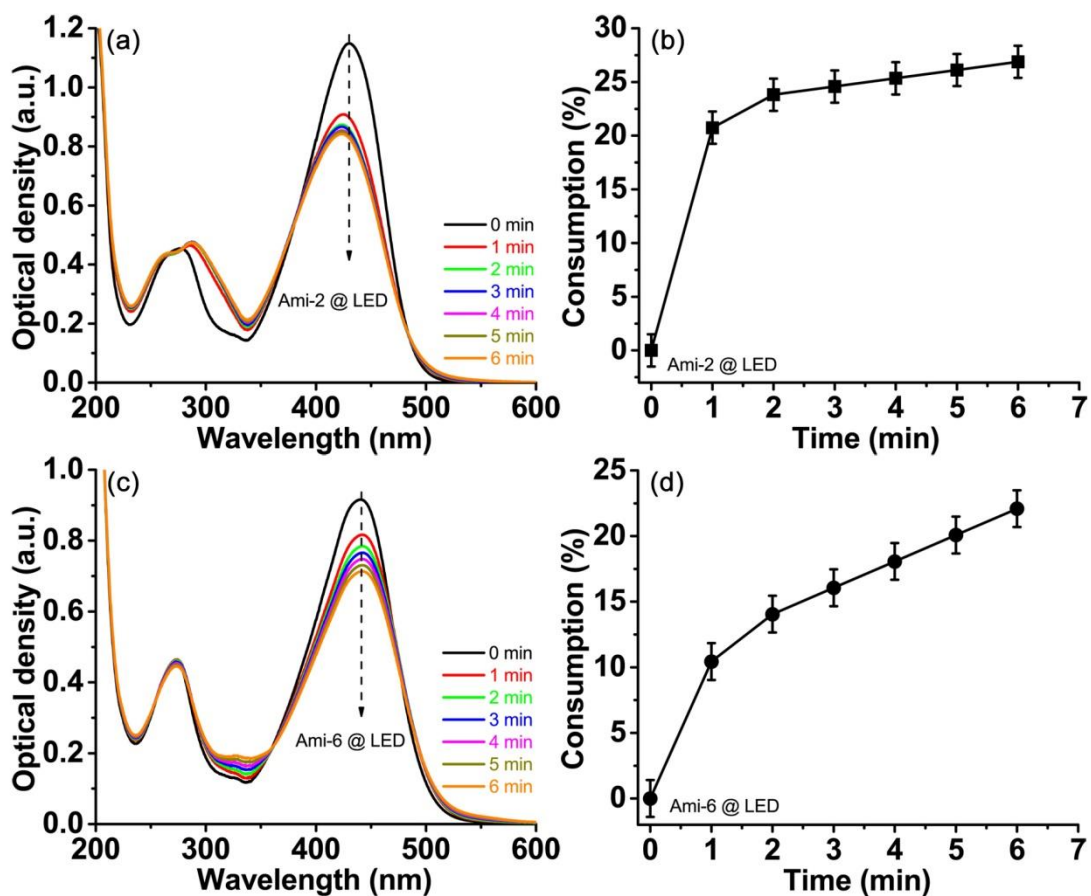


Figure S7 Left: UV-vis absorption spectra of (a) Ami-2 (2.64×10^{-5} M) and (c) Ami-6 (2.21×10^{-5} M) alone in the solvent of acetonitrile upon exposure to LED@405 nm irradiation for 6 min. Right: Consumption of (b) Ami-2 and (d) Ami-6 vs. LED@405 nm irradiation time, respectively.

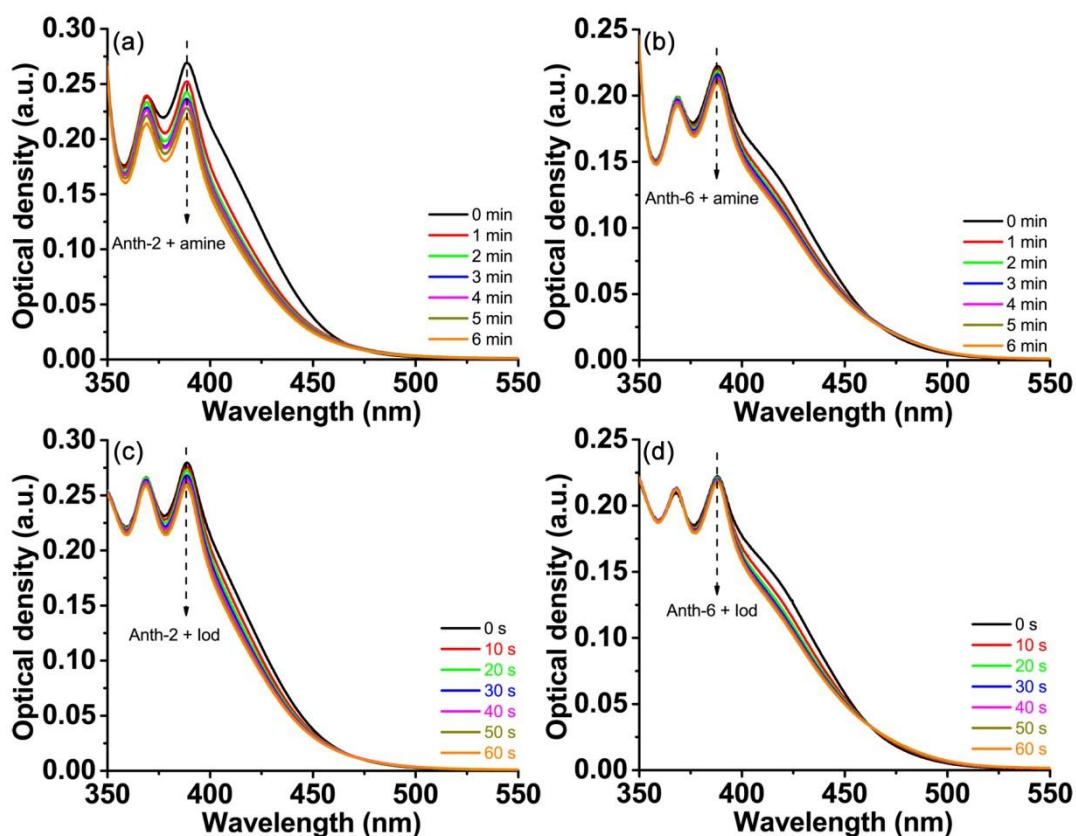


Figure S8 Up: UV-vis absorption spectra of (a) Anth-2 (2.03×10^{-5} M) and (b) Anth-6 (1.77×10^{-5} M) in the presence of amine (EDB, 1.03×10^{-2} M) upon exposure to LED@405 nm irradiation for 6 min. Down: UV-vis absorption spectra of (c) Anth-2 (2.03×10^{-5} M) and (d) Anth-6 (1.77×10^{-5} M) in the presence of iodonium salt (Speedcure 938, 1.03×10^{-2} M) upon exposure to LED@405 nm irradiation for 60 s, respectively. The solvent is acetonitrile.